Phagocyte interactions with *Mycobacterium tuberculosis* – simultaneous analysis of phagocytosis, phagosome maturation and intracellular replication by imaging flow cytometry

Jessika Johansson[1], Anna Karlsson[1], Johan Bylund[2], and Amanda Welin[1]*

[1]Department of Rheumatology and Inflammation Research, Institute of Medicine, Sahlgrenska Academy at University of Gothenburg, Sweden.
[2]Department of Oral Microbiology and Immunology, Institute of Odontology, Sahlgrenska Academy at University of Gothenburg, Sweden.

*Corresponding author:
Amanda Welin, PhD
Address: Department of Rheumatology and Inflammation Research, University of Gothenburg, Guldhedsgatan 10A, SE-41346 Gothenburg, Sweden
Telephone: +46313424671
E-mail: amanda.welin@gu.se

Running title: Imaging flow cytometry of mycobacterial phagosomes

Abbreviations: Albumin dextrose catalase (ADC), channel (Ch), extended depth of field (EDF), fluorescein isothiocyanate (FITC), green fluorescent protein (GFP), lipoarabinomannan (LAM), lysosome-associated membrane glycoprotein (LAMP), phorbol 12-myristate 13-acetate (PMA), phosphate-buffered saline (PBS), root mean square (RMS), tuberculosis (TB).

Abstract

Utilization of compounds that enhance the innate immune response against *M. tuberculosis* is an attractive strategy for combating tuberculosis in the post-antibiotic era. Thus, it is crucial to develop methods that can be used to screen for such compounds and to investigate their mechanisms of action. Here, we used imaging flow cytometry (ImageStreamX Mk II), which enables rapid quantification of microscopic images in flow, to study the interaction between phagocytes and *M. tuberculosis*. Macrophage-differentiated THP-1 cells were infected with GFP-expressing *M. tuberculosis* H37Ra, and methods for rapidly assessing phagocytosis, phagosome maturation, and bacterial replication inside the cells were developed and evaluated. These aspects of innate immunity are essential in determining the outcome of mycobacterial infection of phagocytes. The technique was found effective for monitoring phagocytosis of mycobacteria, phagosomal acidification and phagolysosomal fusion, as well as for measuring mycobacterial replication inside the cells. Several of these aspects could be analyzed simultaneously in the same sample, providing a great deal of information about the phagocyte-mycobacterial interaction at once. Thus, this method has great potential to be useful both for basic research questions and for evaluating compounds that enhance the innate immune response against *M. tuberculosis*.

Key words: ImageStreamX, mycobacteria, phagolysosomal fusion, LysoTracker, CD63, macrophage

1. Introduction

Mycobacterium tuberculosis causes tuberculosis (TB), an infectious disease that kills nearly two million people each year worldwide. The bacterium is transmitted by contaminated aerosols released through coughing, and exposure can lead to a spectrum of outcomes; from clearance by the innate or adaptive immune system, to latent infection or active disease (Barry et al., 2009). The importance of innate immunity in protection against TB is illustrated by the fact that up to 50 % of exposed individuals clear the infection without the onset of adaptive immunity (Morrison et al., 2008; Verrall et al., 2014). New treatment strategies against TB are sorely needed to combat emerging antibiotic resistance, and an attractive approach is to boost the innate immune response in order to enhance bacterial clearance (Verrall et al., 2014).

Following inhalation, *M. tuberculosis* is phagocytosed by alveolar macrophages in which the bacteria inhibit phagosome maturation to grant intracellular survival and replication. Regular phagosome maturation entails the fusion between the phagosome in which the bacterium resides and lysosomes, as well as the acquisition of vacuolar H^+-ATPases leading to a drop in pH and activation of bactericidal proteases originating from the lysosomes (Sturgill-Koszycki et al., 1994; Vergne et al., 2004; Welin and Lerm, 2012). Lysosomal markers such as CD63 (also known as lysosome-associated membrane glycoprotein 3, LAMP-3), LAMP-1, or functional dyes staining acidic compartments can be used to investigate whether phagosome maturation has occurred (Welin et al., 2008; Welin et al., 2011b). The partial arrest of phagosome maturation by *M. tuberculosis* is an active process dependent on the mycobacterial cell wall component lipoarabinomannan (LAM) (Welin et al., 2008; Welin and Lerm, 2012). The LAM causes inhibition of calcium signalling and of a type III PI 3-kinase necessary for the fusion and fission events involved in phagosome maturation (Vergne et al., 2004). It is known that the degree of antibacterial pressure exerted on *M. tuberculosis* inside the phagosome influences the outcome of macrophage infection (Dhiman et al., 2009; Welin et al., 2011b), and mycobacterial mutants defective in the inhibition of phagosome maturation display reduced survival inside murine macrophages (Pethe et al., 2004). Thus, phagosome maturation is a potential target for new drugs that enhance the innate immune response against *M. tuberculosis*.

In order to find compounds that target the innate immune system, boosting bacterial killing inside the macrophage without causing immunopathology, new methods are needed. Current approaches for quantifying phagosome maturation involve laborious microscopy protocols and manual subjective scoring of phagosomes (Welin et al., 2008; O'Leary et al., 2011; Welin et al., 2011a), or advanced functional assays that probe the phagosomal environment (Rohde et al., 2007). Although both have been very valuable in characterizing the mycobacterial compartment, neither is easily adapted to the screening context even on a small scale. Furthermore, rapid and very useful methods for evaluating bacterial growth or killing inside host cells are available (Eklund et al., 2010; Andreu et al., 2012; Kicka et al., 2014), but not in combination with analysis of phagosome maturation or other intracellular phenomena. Here, we developed a new tool for simultaneous quantification of phagocytosis, phagosome maturation, and bacterial replication inside macrophages interacting with *M. tuberculosis*, based on imaging flow cytometry. Imaging flow cytometry combines fluorescence microscopy and flow cytometry, enabling rapid flow-based quantification of fluorescence microscopic image information, and provides many advantages that can be employed in the search for new treatment strategies against TB as well as for basic research.

2. Materials and Methods

2.1 Culture of M. tuberculosis

The avirulent *M. tuberculosis* strain H37Ra (ATCC #25177, Biosafety Level 2) was used for all experiments. Early passages were prepared and stored at −70°C. The bacteria were cultured in Middlebrook 7H9 broth with 0.05 % Tween-80, 0.5 % glycerol and albumin dextrose catalase (ADC) enrichment (BD) at 37°C for 2–4 weeks, and then passaged and incubated for 1 week before use in experiments. For constitutive expression of green fluorescent protein (GFP), H37Ra bacteria were transformed with the pFPV2 plasmid carrying the gene for GFP, and plasmid-carrying mycobacteria were selected using 20 µg/ml kanamycin (Welin et al., 2011a). Heat-killed fluorescein isothiocyanate (FITC)-labeled *M. tuberculosis* H37Ra was prepared by incubation of H37Ra (without the pFPV2 plasmid) in a water bath at 80^{o}C for 1 h, multiple passages through a syringe equipped with a 27-gauge needle, followed by labeling with 2 µg/ml FITC (Sigma) and several washes, and stored at -20^{o}C until use.

2.2 Cell culture

The monocytic cell line THP-1 (ATCC #TIB-202) was cultured by standard procedures in RPMI 1640 supplemented with 10 % fetal calf serum, 2 mM L-glutamine, 100 U/ml penicillin and 100 µg/ml streptomycin (Fisher Scientific). The cells were maintained at 37°C in a humidified atmosphere with 5 % CO_2 and passaged every 3-4 days. For differentiation to macrophage-like cells and use in experiments, THP-1 cells were seeded (1x10^{6}/well) in 6-well plates in fresh medium supplemented with 100 nM phorbol 12-myristate 13-acetate (PMA, Sigma), and incubated for 18 h (Theus et al., 2004). Efficient differentiation was defined as adherence to the plastic. The cells were then allowed to rest in RPMI without PMA for at least 2 h.

2.3 Preparation of phagocytic prey

The H37Ra suspension was washed in phosphate-buffered saline (PBS) supplemented with 0.05 % Tween-80. Single bacilli were obtained by passing the suspension 10 times through a syringe equipped with a 27-gauge needle, a further wash, resuspension in plain RPMI (*i.e.* without additives), and finally another 10 passages through the needle (Welin et al., 2011a). In some experiments, FITC-labeled zymosan particles (Life Technologies) were used as phagocytic prey. The concentration of bacteria and zymosan was determined using an Accuri C6 flow cytometer (BD). Opsonization of bacteria was carried out in Protein LoBind tubes (Eppendorf). For serum opsonization, the phagocytic prey was incubated with normal human serum (Sahlgrenska University Hospital Blood Bank, 25 % or 50 % as stated), at 37^{o}C for 30 min. For IgG opsonization of mycobacteria, the bacilli were incubated with 20 µg/ml polyclonal rabbit anti-*M. tuberculosis* antibody (Abcam ab905), after removal of sodium azide from the buffer using protein G-coated Dynabeads® (Life Technologies), under the same conditions. The prey was not washed after opsonization.

2.4 Infection of cells

Adherent THP-1 cells were washed in plain RPMI to remove serum and antibiotics, and the phagocytic prey was added at the indicated ratio (prey:cells), diluted in plain RPMI. Synchronization of phagocytosis was achieved by centrifugation of the plate (3000 ×g, 5

min), after which the plate was incubated at 37°C for 2 h or the indicated time. For long-term incubations over several days, the medium was exchanged after 2 h for RPMI supplemented with 10 % fetal calf serum and 2 mM L-glutamine, with or without the addition of antimycobacterial antibiotics (100 µg/ml streptomycin) as stated.

2.5 LysoTracker and CD63 staining

For staining of acidified compartments in THP-1 cells, LysoTracker® Deep Red (Life Technologies) at 75 nM was added to the medium during the final 20 min of infection (Welin et al., 2011a). LysoTracker stains compartments with a pH of about 6 and below (von Bargen et al., 2009), and the *M. tuberculosis*-containing phagosome has an average pH of about 6.4, as opposed to a mature phagosome with a pH of less than 5 (Rohde et al., 2007), making LysoTracker an appropriate probe. The cells were removed from the surface using a cell scraper following incubation with lidocaine hydrochloride monohydrate (Sigma, 4 mg/ml) at 37°C for 15 min, and washed with PBS by centrifugation (500 ×g, 5 min). LysoTracker-stained cells were then resuspended in 25 µl PBS and placed on ice for immediate imaging flow cytometry analysis. CD63 was used as a late endosomal/lysosomal marker (Welin et al., 2011a). Indirect intracellular immunofluorescence staining of detached, fixed, and permeabilized cells was performed as previously described (Welin et al., 2013), using a monoclonal mouse-anti human CD63 antibody (Sanquin, 4 µg/ml) followed by an Alexa Fluor 647-conjugated goat anti-mouse ($F(ab')_2$ fragment) secondary antibody (Life Technologies, 2.5 µg/ml). Cells were washed and resuspended in 25 µl PBS before analysis by imaging flow cytometry.

2.6 Imaging flow cytometry

All samples were analyzed using an ImageStreamX Mk II imaging flow cytometer (Amnis), followed by IDEAS analysis software (v. 6.1, Amnis) as described in section 3 below. The ImageStreamX simultaneously collects six multi-mode images of each event in flow, including brightfield, darkfield (corresponding to side scatter) and up to four fluorescence colors. Images are then analyzed using IDEAS software, enabling quantification of different aspects of the obtained image data. A "mask" defines the region of interest in the cell, and quantification of different parameters inside the mask is then performed using a "feature", which can be custom-made. Here, the 488 nm laser was used for excitation of GFP or FITC and the 642 nm laser for excitation of Alexa Fluor 647 or LysoTracker Deep Red. The 60X magnification objective was used, providing a pixel size of 0.33 μm^2 and a depth of field of 2.5 µm. 20 000 events were collected per sample (at a speed of about 50-150 cells per second), ensuring a sufficient number of events remaining for statistically robust analysis after all the gating steps (generally above 500 cells). Single stain samples were routinely collected using the same settings and used as compensation controls to generate compensation matrices in IDEAS. The extended depth of field (EDF) option on the ImageStreamX can be used to project structures in a wide focal range into one focused image. This option improves accurate enumeration of intracellular spots (Ortyn et al., 2007), such as bacteria, and was used for the bacterial enumeration assay. For the phagosome maturation assay, on the other hand, the EDF option was not used as it could result in false-positive colocalization of prey and lysosomal marker in cells with lysosomes in the same XY location but different focal planes. Maximum data output can be obtained on the ImageStreamX from a limited number of samples if the same samples are run twice, both with and without the EDF option.

2.7 Statistical analysis

Statistical analysis was performed using Graph Pad Prism v. 6.01 (GraphPad Software), as stated in the figure legends. Statistically significant differences are indicated in the figures by a single asterisk (*; P = ≤0.05), double asterisks (**; P = ≤0.01), or triple asterisks (***; P = ≤0.001). The numbers of independent experiments (performed on different days) are stated in the figure legends.

3. Results and Discussion

3.1 Analysis of phagocytosis

Firstly, a method for investigating the efficiency of macrophage phagocytosis was developed, as phagocytosis is a key component of innate immunity in TB (Verrall et al., 2014). The assay was based on a setup where macrophage-differentiated THP-1 cells were allowed to phagocytose zymosan particles or *M. tuberculosis*, followed by staining of a lysosomal marker and imaging flow cytometry analysis.

3.1.1 IDEAS analysis

In order to quantify what proportion of the cells had phagocytosed *M. tuberculosis*, a four-step gating strategy was developed (Fig. 1). This method was very similar to the built-in internalization wizard in IDEAS, and was performed essentially as described by others (Phanse et al., 2012). First, the gradient RMS (root mean square for image sharpness) feature in the brightfield channel (Ch04) was used to gate in-focus cells, followed by identification of single cells using the area and aspect ratio features in the brightfield image. Then, events that were positive for at least one phagocytic prey were gated based on the intensity and max pixel feature values in the GFP/FITC channel (Ch02). The background lysosomal (LysoTracker or CD63, Ch05) staining (the default M05 mask eroded by 4 pixels) defined the boundaries of the cell cytoplasm, and the internalization feature (the log-transformed ratio of the background-subtracted GFP/FITC intensity inside the cell boundaries to the total background-subtracted GFP/FITC intensity) was used to determine whether the phagocytic prey was internalized or merely bound to the cell surface. Cells with values above zero were considered as having internalized prey, and this was confirmed by visual inspection of numerous images from several experiments. The cells were thus categorized into having no prey association, prey bound to the cell surface, or internalized prey. It is noteworthy that a cell containing both surface-bound and internalized prey, or prey located on the mask border, will result in intermediate internalization scores, which can lead to misclassification of a small number of events.

3.1.2 Phagocytosis measurements

The phagocytosis assay was evaluated in several different experimental setups. It is well known that opsonization of phagocytic prey with serum leads to enhanced uptake, through complement components C3b and iC3b interacting with phagocyte complement receptors, and that opsonization with prey-specific IgG leads to enhanced uptake through Fcγ receptors (Aderem and Underhill, 1999). Thus, opsonization was used to confirm that differences in phagocytic uptake could be detected by our method. First, the cells were allowed to phagocytose unopsonized or serum-opsonized FITC-labeled zymosan particles at a ratio of 1:1 for 2 h. Opsonization resulted in a significantly increased degree of zymosan internalization (Fig. 2A). We assumed that this was mainly due to increased engagement of complement receptors, but as the BCG statuses of the serum donors were not known there might also have been an element of antibody opsonization. Next, the cells were allowed to interact with serum-opsonized zymosan at a ratio of 1:1 for different periods of time. Successively increased phagocytic uptake could be observed over time (Fig. 2B), although there was little increase beyond 1 h of incubation. Finally, *M. tuberculosis* H37Ra (expressing GFP) was used as phagocytic prey at a ratio of 2:1. Opsonization with either serum or anti-*M. tuberculosis* IgG significantly enhanced phagocytic uptake after 2 h (Fig. 2C). Further,

increasing the prey:cells ratio to 2:1 or 6:1 resulted in successively more phagocytic uptake as compared to ratio 1:1 (data not shown). All the statistically significant differences were found in internalization of prey, while no differences were found in the levels of surface-bound prey.

3.1.3 Discussion

The described method was shown to be effective in assessing the degree of uptake of different phagocytic prey, including *M. tuberculosis*, and had the advantage of being flow-based and thus rapid as well as quantitative. Another advantage is that the method does not require any special stains or treatments to determine whether prey is internalized or surface-bound, since this property is built into the IDEAS analysis. The only requirement is that the cell contains a stain that can be used to define its boundaries. Although the lysosomal markers used here are not conventionally used to define cell boundaries, the fact that they both produced a slight background staining of the entire cell area, likely due to unspecific binding, meant that they could be utilized for this purpose. Other ways of determining binding versus internalization of phagocytic prey is through chemical extinction of fluorescence arising from extracellular bacteria (Giaimis et al., 1994), antibody staining of extracellular bacteria on non-permeabilized cells (Johnson and Criss, 2013), or incubation with pharmacological agents that inhibit the polymerization of actin and thus internalization of phagocytic prey (Keller and Niggli, 1995), all of which are more laborious. Using the extended depth of field (EDF) option could enhance the accuracy of the phagocytosis analysis, as this would include bacteria in all focal planes of the images, but this strategy has the disadvantage of not being able to distinguish between surface-bound and internalized prey, and would furthermore not be compatible with simultaneous analysis of phagosome maturation (described under 3.2 below) in the same data file.

3.2 Analysis of phagosome maturation

Secondly, a method for analysis of phagosome maturation in *M. tuberculosis*-infected macrophages was developed, as phagosome maturation may be a potential target for new immune-boosting treatment strategies against TB. It is well-known that live *M. tuberculosis* actively inhibits phagosomal acidification and fusion with lysosomes (Armstrong and Hart, 1971; Clemens and Horwitz, 1995; Via et al., 1997; Lee et al., 2008a; Welin et al., 2011a), and that this immune evasion mechanism is essential for intracellular survival and replication of the bacteria (Pethe et al., 2004; Dhiman et al., 2009; Welin et al., 2011b). On the other hand, both virulent strains such as H37Rv and avirulent strains such as H37Ra are capable of inhibiting phagosome maturation (Lee et al., 2008b; Eklund et al., 2010; Welin et al., 2011a), demonstrating that this trait is not the sole determinant of the ability to replicate inside macrophages. Adaptation to the intraphagosomal environment (Russell, 2011) as well as escape from the phagosome into the cytosol (van der Wel et al., 2007; Houben et al., 2012) are also needed, and the inhibition of phagosome maturation thus represents only part of the arsenal of immune evasion strategies employed by *M. tuberculosis*. In order to enable small-scale screening for compounds that enhance phagosome maturation in *M. tuberculosis*-infected macrophages, we developed two different analysis strategies for rapidly quantifying phagosome maturation by imaging flow cytometry, described below. Both were based on experiments where macrophage-differentiated THP-1 cells were allowed to phagocytose *M. tuberculosis* H37Ra, followed by staining of a lysosomal marker and imaging flow cytometry analysis. We primarily used LysoTracker as a lysosomal marker for these assays. LysoTracker is an excellent tool for tracking acidic compartments, but it is not compatible with fixation and permeabilization of the cells, which may be desirable. In particular, if the

assays are to be carried out using virulent strains of *M. tuberculosis*, which are Biosafety Level 3, it is necessary to either fix the samples or house the imaging flow cytometer inside a Biosafety Level 3 facility. Thus, we also evaluated phagosome maturation using the lysosomal membrane marker CD63 which is compatible with fixation.

3.2.1 IDEAS analysis

3.2.1.1 Phagosome maturation score

As mentioned, two different analysis strategies were employed to investigate phagosome maturation, each with different advantages making them suitable for different applications. The first strategy was a custom-made IDEAS analysis that could classify a cell as containing a mature or an immature phagosome. The analysis essentially quantifies the extent to which the lysosomal marker is enriched in the phagosome as compared to the rest of the cell. We termed the feature used for this analysis "phagosome maturation score."

Upon analysis of phagocytosis as described in section 3.1.1 above, further gating was performed on the cells with internalized phagocytic prey to identify those that could be analyzed for phagosome maturation using the phagosome maturation score (Fig. 3A). First, the gradient RMS feature in the GFP/FITC channel (Ch02) was used to gate cells where the prey was in focus. This was required as the ImageStreamX (without the EDF option) provides a limited depth of field (2.5 µm at 60X), meaning that some phagosomes will be out of focus. Then, it was necessary to identify the cells that contained only one phagosome. This is because flow-based techniques such as this one provide quantification on an event level (*i.e.* for the entire cell), rather than for each individual phagosome. Thus, it is not possible to score a cell containing multiple phagosomes as positive or negative for phagosome maturation. The infection protocol (using a low prey:cell ratio of 1-2:1) was optimized to provide a sufficient number of events with only one phagosome in this final gating step. To identify cells containing a single phagosome, the shape ratio feature (the minimum thickness divided by the length) of the Ch02 object mask was used, where a low value signifies an elongated and uneven mask while a high value indicates a mask with rounder shape, *i.e.* a single phagosome. Cells with multiple phagosomes were thus excluded in this step. The gate was set so that cells where the single phagosome was either rod-shaped or round were included. This was because *M. tuberculosis* is a rod-shaped bacillus, meaning that the mask will be rod-shaped if a phagosome containing one bacillus is imaged from the side. However, the mask can also be round if a phagosome containing one bacillus is imaged in cross-section, or if there are more than one bacillus in the same phagosome. Thus, only single phagosomes were included, but these were allowed to contain one or more bacilli.

A custom-made masking and feature strategy was subsequently employed to identify the cells in which the LysoTracker or CD63 staining (Ch05) was elevated in the phagosome as compared to the rest of the cell, indicating phagosome maturation (Fig. 3B). First, a mask defining the phagosome was created, covering the Ch02 object mask dilated by two pixels. The dilation of the mask was performed to also enable analysis of phagosomes containing prey that is larger than the depth of field of the ImageStreamX, such as zymosan, where phagosome maturation results in a ring of lysosomal marker around the prey rather than in colocalization. The remainder of the cell was defined as the Ch05 object mask minus ("and not" in the equation below) this phagosome mask. Then, the mean pixel value of LysoTracker or CD63 in the phagosome mask was divided by the mean pixel value of LysoTracker or CD63 in the remaining cell mask. This yielded a phagosome maturation score for each cell,

where values above 1 indicate enrichment of LysoTracker staining (Fig. 3C) or CD63 (Fig. 3D) in the phagosome as compared to the rest of the cell. The definition of the feature was thus as follows:

Phagosome maturation score = Mean Pixel_Dilate(Object(M02, Ch02, Tight), 2)_Ch05 / Mean Pixel_Object(M05, Ch05, Tight) And Not Dilate(Object(M02, Ch02, Tight), 2)_Ch05

After visual inspection of numerous images from several experiments, the limit for positive phagosome maturation was set to 1.5. Since this analysis strategy is based on the mean rather than the total intensity of the lysosomal marker in the masks, it is indifferent to the size of the phagosome and cell, and the use of a ratio makes it indifferent to the total intensity of lysosomal marker in the cell. However, it is inevitable that some cells with an intermediately mature phagosome in a real sample will be difficult to classify, and that some cells with a non-phagosomal bright patch of LysoTracker in addition to an acidified phagosome will result in false negatives. In order to validate our method, it was compared to the well-established method of quantifying phagosome maturation in microscopy images (Welin et al., 2008; O'Leary et al., 2011; Welin et al., 2011a), using the images obtained using ImageStreamX. The proportion of cells with a mature phagosome as determined by the phagosome maturation score was compared to that obtained by manual scoring of the first 100 cells containing a single phagosome in 3 independent experiments where THP-1 cells had been infected with live unopsonized H37Ra-GFP and stained with LysoTracker. The two methods of quantification yielded almost identical results (Fig. 3E), demonstrating that the phagosome maturation score could effectively discriminate between cells with and without enrichment of lysosomal markers in the phagosome.

3.2.1.2 Colocalization

The second strategy for analyzing phagosome maturation was based on the built-in IDEAS wizard analysis for colocalization, which has been used by others to study the colocalization of different phagosome markers (Ploppa et al., 2011; Smirnov et al., 2015). This wizard measures the degree to which two probes with punctate staining spatially colocalize in the images, and uses the bright detail similarity R3 feature (the log transformed Pearson's correlation coefficient of the localized bright spots with a radius of 3 pixels or less in two images). This analysis was performed after gating as described for the phagosome maturation score in section 3.2.1.1, apart from the last step identifying cells with a single phagosome. This step was left out as the colocalization analysis does not require a mask defining the phagosome, but rather considers bright spots in the entire image, and can thus handle cells containing multiple phagosomes with different degrees of maturation (yielding an intermediate bright detail similarity score). Typical results and example images are shown in Fig. 4. As the strategy based on colocalization includes cells with multiple phagosomes, it was not possible to classify each cell into "mature" or "not mature," but rather the median bright detail similarity scores were compared between different samples. For this reason, a validation as shown for the phagosome maturation score in Fig. 3E was not possible here. Further, the fact that not all the lysosomes in a cell translocate to the phagosomes during phagosome maturation means that complete colocalization between phagocytic prey and lysosomal marker will not be achieved, but rather varying degrees of colocalization.

3.2.2 Phagosome maturation measurements

In order to evaluate these imaging flow cytometry-based phagosome maturation assays, they were employed to analyze the degree of phagosome maturation using different prey and

opsonization conditions. We started by evaluating phagosome maturation using LysoTracker. Macrophage-differentiated THP-1 cells were infected with live GFP-expressing H37Ra or heat-killed and FITC-labeled H37Ra at a ratio of 2:1 for 2 h, and stained with LysoTracker. First, the phagosome maturation score was used for analysis. It was clear that the method was capable of detecting differences between the live and dead bacilli in the ability to inhibit phagosomal acidification (Fig. 5A, left panel), and the results were in line with previous results obtained using conventional confocal microscopy methods (Welin et al., 2011a). Furthermore, very similar results were obtained when the colocalization analysis was applied instead (Fig. 5A, right panel), demonstrating that this strategy was also useful in detecting differences in phagosome maturation in this context.

Conflicting data exist concerning whether the receptors engaged during phagocytosis of *M. tuberculosis* can influence the degree of phagosome maturation and the outcome of infection. There are examples of studies showing that uptake through complement receptor 3 can be advantageous for the bacillus (Caron and Hall, 1998; Ernst, 1998), and others showing that uptake through this receptor makes no difference to phagosome maturation or bacterial replication (Zimmerli et al., 1996; Hu et al., 2000). It has been shown that uptake of mycobacteria through Fcγ receptors can lead to enhanced phagosome maturation and a more pro-inflammatory macrophage response (Armstrong and Hart, 1975; Caron and Hall, 1998; de Valliere et al., 2005). However, our imaging flow cytometry-based analysis of phagosome maturation, using LysoTracker staining and the phagosome maturation score, showed no enhancement of LysoTracker enrichment and thus acidification and phagosome maturation when mainly Fcγ or mainly complement receptors were engaged for H37Ra uptake (Fig. 5B, left panel). Again, a similar trend was obtained when the same data were analyzed using the colocalization approach (Fig. 5B, right panel).

Next, in order to evaluate phagosome maturation using the lysosomal membrane marker CD63, the use of which permits fixation of samples, we allowed THP-1 cells to ingest FITC-labeled zymosan particles for different periods of time and stained the cells for CD63 after fixation and permeabilization. As shown in Fig. 5C, this protocol resulted in a successive increase in translocation of CD63 to the zymosan-containing phagosome, as analyzed using the phagosome maturation score. When FITC-labeled zymosan was compared to GFP-expressing H37Ra as phagocytic prey, and infection at a ratio of 1:1 was allowed to proceed for 2 h, a difference in phagosome maturation between cells infected with the two types of prey could also be detected (Fig. 5D), as expected. Thus, the presented assay could efficiently detect differences in phagosome maturation using two different markers.

3.2.3 Discussion

The two described approaches to analyzing phagosome maturation have different advantages and disadvantages, each explained in more technical detail in section 3.2.1 above. The approach based on phagosome maturation score (*i.e.* analyzing the extent to which the lysosomal marker is enriched in the phagosome) can only handle cells containing a single phagosome, which can be problematic if the investigated compound acts as an opsonin that influences the number of phagosomes per cell, in which case the analysis will be skewed. On the other hand, it has the advantage of providing a percentage of cells with mature phagosomes rather than an arbitrary score, and is capable of analyzing cells containing large prey where phagosome maturation results in a ring of lysosomal marker around the prey rather than in colocalization. The approach based on colocalization (*i.e.* analyzing the degree to which the fluorescence signal from the prey and the lysosomal marker spatially colocalize),

on the other hand, can handle cells containing multiple phagosomes, but provides only an arbitrary score and is not capable of analyzing larger phagosomes containing *e.g.* zymosan. Thus, depending on the experiment, it may be appropriate to choose one approach over the other.

A previous study showed that LysoTracker staining of the phagosome better correlates with the ability of macrophages to inhibit intracellular replication of *M. tuberculosis* than does the translocation of CD63, as acidification reflects the functional state of the phagosome better than membrane markers do (Welin et al., 2011a). Further, replication of virulent *M. tuberculosis* inside CD63-positive phagosomes has been shown (van der Wel et al., 2007; Welin et al., 2011a), and the ability of *M. tuberculosis* to inhibit acidification correlates better with metabolic activity of the bacteria than does the ability to inhibit recruitment of CD63 to the phagosome (Lee et al., 2008a). Others have also questioned the use of CD63 as a marker of truly mature phagosomes due to its presence on intermediate/late endosomes in addition to lysosomes (Sturgill-Koszycki et al., 1994; Rohde et al., 2007), and it has been suggested that phagolysosomal fusion and the recruitment of vacuolar H+-ATPases occur through different mechanisms (Fratti et al., 2003; Vergne et al., 2004; Kinchen and Ravichandran, 2008; Sun-Wada et al., 2009; Welin et al., 2011a). Thus, the LysoTracker approach may be more suitable, although the CD63 approach allows fixation of samples, which is desirable if working with virulent mycobacteria. The presented assay could potentially be modified for other endosomal and functional markers in order to study intracellular trafficking in different respects. LysoTracker Deep Red could also be replaced by a dye that stains acidic compartments and is compatible with fixation. Further, it can be adapted for markers of autophagy, a process shown to be important for enhancing phagosome maturation in *M. tuberculosis*-infected macrophages (Gutierrez et al., 2004; Purdy, 2011) and which has previously been quantified by imaging flow cytometry (Demishtein et al., 2015).

3.3 Analysis of bacterial numbers

Finally, we developed an imaging flow cytometry-based method for analyzing intracellular replication of *M. tuberculosis* inside macrophages. Measuring intracellular replication rates is an essential component of evaluating the effect of different compounds on the outcome of mycobacterial infection. It is important that new anti-mycobacterial compounds act inside macrophages as this is the main site of infection, and a useful screening method should thus include the host cell. The assay employed macrophage-differentiated THP-1 cells infected with H37Ra-GFP for different periods of time in the presence or absence of antibiotics.

3.3.1 IDEAS analysis

In order to accurately enumerate intracellular bacteria, samples were collected using the EDF option, yielding images where bacteria from all focal planes in the cell are projected (Ortyn et al., 2007). A masking strategy to identify individual bacteria in the images was then developed (Fig. 6A) with the aid of the built-in spot counting wizard in IDEAS, and by visual inspection of numerous images in each step to confirm validity of the masks. First, all bright regions of the Ch02 prey image were masked using the spot mask, setting the spot to cell background ratio to 2 and the radius to 3. Then, to distinguish bacteria that were very close to each other, a peak mask (identifying local intensity maxima) was applied, setting the spot to background ratio to 1. Finally, an intensity mask was applied to remove very dim spots that were the result of cellular autofluorescence (based on inspection of uninfected cells),

restricting the intensity to 80-4095 counts. The spot count feature was then applied in this mask, making the definition of the bacterial count feature as follows:

Bacterial count = Spot Count_Intensity (Peak(Spot(M02, Ch02, Bright, 2, 3), Ch02, Bright, 1), Ch02, 80-4095)

Fig. 6B shows an example of this analysis applied to cells that were determined by the analysis of phagocytosis (described in section 3.1.1 and shown in Fig. 1 steps 1-3) to be positive for phagocytic prey. Cells that were determined by the bacterial count feature to contain 0, 1, 2, or 3 bacteria are depicted. This bacterial enumeration analysis can be applied to all single cells in order to analyze the average number of bacteria per cell, which would be desirable in an intracellular killing or replication assay. Alternatively, the analysis can be applied only to the cells that are positive for phagocytic prey, *e.g.* to accurately determine the efficiency of phagocytic uptake.

The method was validated by comparing it to manual counting of the number of bacteria per cell in the ImageStreamX images. The number of bacteria was counted in the first 300 cells that were positive for prey in an experiment where THP-1 cells had been infected with live unopsonized H37Ra-GFP for 2 h. Manual counting (Fig. 6C) yielded a similar frequency distribution to that obtained using the bacterial count feature (compare to Fig. 6B). Notably, it was very difficult to accurately distinguish single bacteria by eye in cells infected with multiple bacteria or bacterial aggregates, possibly leading to an underestimation of the number of bacteria by this method. This was reflected by the slightly lower mean number of bacteria per cell as determined by manual counting (3.1 bacteria per cell) than that achieved using the bacterial count feature (3.5 bacteria per cell) in this sample. The validation showed that the presented method was accurate in determining the number of mycobacteria per cell.

3.3.2 Intracellular bacterial replication measurements

In order to evaluate the bacterial enumeration method, we infected macrophage-differentiated THP-1 cells with GFP-expressing H37Ra for different periods of time, with and without the addition of streptomycin. Streptomycin is an aminoglycoside antibiotic with well-documented antimycobacterial effects inside macrophages that leads to the inhibition of intracellular bacterial replication (Eklund et al., 2010). Cells were fixed and stained for CD63, and analyzed by imaging flow cytometry using the EDF option to obtain images where all the bacteria in each cell were projected into one image. The reason for using CD63 was to enable storage of fixed samples and acquisition of several data points at once, but CD63 and LysoTracker could be used interchangeably for this assay. H37Ra replicated slightly inside the cells, increasing from a mean of 1.4 bacteria per cell to 4.5 bacteria per cell over 4 days (Fig. 7). This intracellular replication rate of H37Ra is similar to previously published data using either manual counting (Welin et al., 2011a) or luciferase-based measurements (Eklund et al., 2010) of H37Ra inside human monocyte-derived macrophages, and represents a much lower intracellular replication ability than that of the virulent strain H37Rv (Eklund et al., 2010; Welin et al., 2011a). The replication rate presented here is slightly higher than that reported previously, probably representing a lower ability of differentiated THP-1 cells to control mycobacterial replication as compared to monocyte-derived macrophages. The presence of streptomycin resulted in a significantly reduced number of bacteria per cell, only doubling over 4 days (Fig. 7). This demonstrates that the method was useful for determining differences in intracellular bacterial replication.

3.3.3 Discussion

The presented approach proved effective in measuring intracellular growth of *M. tuberculosis*, and could potentially be adapted for many applications, including small-scale screening of compounds that are suspected to inhibit mycobacterial growth inside host cells by either activating the cells or by killing the bacteria directly. If required, phagosome maturation could be analyzed in the same samples that are analyzed for bacterial numbers, if additional images are acquired without the EDF option. This is because analysis of phagosome maturation using the EDF option can result in false positives, as discussed in section 2.6 above. Acquiring the same samples twice, both with and without the EDF option, maximizes the amount of information that can be extracted from one sample. Further, it would be possible to combine the described bacterial enumeration method with a stain that determines whether the host cell is viable, which may be desirable as virulent *M. tuberculosis* is known to induce necrosis in the host macrophage (Eklund et al., 2010; Welin et al., 2011a). The stability of GFP means that it may be difficult to detect actual killing of the bacteria, as the signal may remain for long periods of time even if the bacteria have been killed. However, the assay was demonstrated to be very useful for detecting differences in bacterial numbers and thus replication rates inside the host cell, which in the screening context could be the result of either inhibited replication or bacterial killing.

4. Conclusions

We conclude that the presented imaging flow cytometry-based methods are effective for measuring phagocytosis, phagosome maturation, and intracellular growth of *M. tuberculosis* in macrophage-differentiated THP-1 cells. The assays could potentially be adapted for other host cell types and bacterial species, as well as for mixed cell populations distinguished by different surface markers. The presented methods have several advantages in that they are quantitative, avoiding the potential bias associated with manual analysis of microscopic images, and rapid, as analysis is carried out in flow. Furthermore, the experimental procedures are routine and analysis is simple once the parameters in IDEAS have been set up once. Above all, however, the methods allow vast amounts of information to be extracted from only a limited number of samples, especially if the samples are run both with and without the EDF option on the ImageStreamX. Fig. 8 summarizes the workflow and the range of analyses that can be performed, demonstrating this fact. Since a great deal of information about the effect of a compound on *M. tuberculosis* infection of macrophages can be extracted from an experiment at once, this novel method is attractive for many basic science applications as well as for small-scale screening of limited numbers of compounds, or for investigating the mechanisms of action of compounds found by other methods to be of interest. The discovery of compounds that enhance the antimycobacterial macrophage response may prove very valuable in combating TB, by complementing existing antibiotics.

5. Acknowledgements

This study was supported by the Swedish Heart-Lung Foundation (#20130442), the Swedish Research Council (#2014-3259 and #2014-396), the King Gustaf V Memorial Foundation, the IngaBritt and Arne Lundberg Research Foundation, the Clas Groschinsky Foundation, and the Swedish state under the ALF agreement.

6. References

Aderem, A. and Underhill, D.M., 1999, Mechanisms of phagocytosis in macrophages. Annual review of immunology 17, 593-623.

Andreu, N., Fletcher, T., Krishnan, N., Wiles, S. and Robertson, B.D., 2012, Rapid measurement of antituberculosis drug activity in vitro and in macrophages using bioluminescence. The Journal of antimicrobial chemotherapy 67, 404-14.

Armstrong, J.A. and Hart, P.D., 1971, Response of cultured macrophages to Mycobacterium tuberculosis, with observations on fusion of lysosomes with phagosomes. J Exp Med 134, 713-40.

Armstrong, J.A. and Hart, P.D., 1975, Phagosome-lysosome interactions in cultured macrophages infected with virulent tubercle bacilli. Reversal of the usual nonfusion pattern and observations on bacterial survival. J Exp Med 142, 1-16.

Barry, C.E., 3rd, Boshoff, H.I., Dartois, V., Dick, T., Ehrt, S., Flynn, J., Schnappinger, D., Wilkinson, R.J. and Young, D., 2009, The spectrum of latent tuberculosis: rethinking the biology and intervention strategies. Nature reviews. Microbiology 7, 845-55.

Caron, E. and Hall, A., 1998, Identification of Two Distinct Mechanisms of Phagocytosis Controlled by Different Rho GTPases. Science 282, 1717-1721.

Clemens, D.L. and Horwitz, M.A., 1995, Characterization of the Mycobacterium tuberculosis phagosome and evidence that phagosomal maturation is inhibited. J Exp Med 181, 257-70.

de Valliere, S., Abate, G., Blazevic, A., Heuertz, R.M. and Hoft, D.F., 2005, Enhancement of innate and cell-mediated immunity by antimycobacterial antibodies. Infection and immunity 73, 6711-20.

Demishtein, A., Porat, Z., Elazar, Z. and Shvets, E., 2015, Applications of flow cytometry for measurement of autophagy. Methods 75, 87-95.

Dhiman, R., Indramohan, M., Barnes, P.F., Nayak, R.C., Paidipally, P., Rao, L.V. and Vankayalapati, R., 2009, IL-22 produced by human NK cells inhibits growth of Mycobacterium tuberculosis by enhancing phagolysosomal fusion. Journal of immunology 183, 6639-45.

Eklund, D., Welin, A., Schon, T., Stendahl, O., Huygen, K. and Lerm, M., 2010, Validation of a medium-throughput method for evaluation of intracellular growth of Mycobacterium tuberculosis. Clinical and vaccine immunology : CVI 17, 513-7.

Ernst, J.D., 1998, Macrophage receptors for Mycobacterium tuberculosis. Infection and immunity 66, 1277-81.

Fratti, R.A., Chua, J., Vergne, I. and Deretic, V., 2003, Mycobacterium tuberculosis glycosylated phosphatidylinositol causes phagosome maturation arrest. Proceedings of the National Academy of Sciences of the United States of America 100, 5437-42.

Giaimis, J., Lombard, Y., Poindron, P. and Muller, C.D., 1994, Flow cytometry distinction between adherent and phagocytized yeast particles. Cytometry 17, 173-8.

Gutierrez, M.G., Master, S.S., Singh, S.B., Taylor, G.A., Colombo, M.I. and Deretic, V., 2004, Autophagy is a defense mechanism inhibiting BCG and Mycobacterium tuberculosis survival in infected macrophages. Cell 119, 753-66.

Houben, D., Demangel, C., van Ingen, J., Perez, J., Baldeon, L., Abdallah, A.M., Caleechurn, L., Bottai, D., van Zon, M., de Punder, K., van der Laan, T., Kant, A., Bossers-de Vries, R., Willemsen, P., Bitter, W., van Soolingen, D., Brosch, R., van der Wel, N. and Peters, P.J., 2012, ESX-1-mediated translocation to the cytosol controls virulence of mycobacteria. Cellular microbiology 14, 1287-98.

Hu, C., Mayadas-Norton, T., Tanaka, K., Chan, J. and Salgame, P., 2000, Mycobacterium tuberculosis infection in complement receptor 3-deficient mice. Journal of immunology 165, 2596-602.

Johnson, M.B. and Criss, A.K., 2013, Fluorescence microscopy methods for determining the viability of bacteria in association with mammalian cells. Journal of visualized experiments : JoVE.

Keller, H. and Niggli, V., 1995, Effects of cytochalasin D on shape and fluid pinocytosis in human neutrophils as related to cytoskeletal changes (actin, alpha-actinin and microtubules). European journal of cell biology 66, 157-64.

Kicka, S., Trofimov, V., Harrison, C., Ouertatani-Sakouhi, H., McKinney, J., Scapozza, L., Hilbi, H., Cosson, P. and Soldati, T., 2014, Establishment and validation of whole-cell based

fluorescence assays to identify anti-mycobacterial compounds using the Acanthamoeba castellanii-Mycobacterium marinum host-pathogen system. PloS one 9, e87834.
Kinchen, J.M. and Ravichandran, K.S., 2008, Phagosome maturation: going through the acid test. Nat Rev Mol Cell Biol 9, 781-95.
Lee, B.Y., Clemens, D.L. and Horwitz, M.A., 2008a, The metabolic activity of Mycobacterium tuberculosis, assessed by use of a novel inducible GFP expression system, correlates with its capacity to inhibit phagosomal maturation and acidification in human macrophages. Molecular microbiology 68, 1047-60.
Lee, J.S., Krause, R., Schreiber, J., Mollenkopf, H.J., Kowall, J., Stein, R., Jeon, B.Y., Kwak, J.Y., Song, M.K., Patron, J.P., Jorg, S., Roh, K., Cho, S.N. and Kaufmann, S.H., 2008b, Mutation in the transcriptional regulator PhoP contributes to avirulence of Mycobacterium tuberculosis H37Ra strain. Cell host & microbe 3, 97-103.
Morrison, J., Pai, M. and Hopewell, P.C., 2008, Tuberculosis and latent tuberculosis infection in close contacts of people with pulmonary tuberculosis in low-income and middle-income countries: a systematic review and meta-analysis. Lancet Infect Dis 8, 359-68.
O'Leary, S., O'Sullivan, M.P. and Keane, J., 2011, IL-10 Blocks Phagosome Maturation in Mycobacterium tuberculosis-infected Human Macrophages. Am J Respir Cell Mol Biol.
Ortyn, W.E., Perry, D.J., Venkatachalam, V., Liang, L., Hall, B.E., Frost, K. and Basiji, D.A., 2007, Extended depth of field imaging for high speed cell analysis. Cytometry. Part A : the journal of the International Society for Analytical Cytology 71, 215-31.
Pethe, K., Swenson, D.L., Alonso, S., Anderson, J., Wang, C. and Russell, D.G., 2004, Isolation of Mycobacterium tuberculosis mutants defective in the arrest of phagosome maturation. Proceedings of the National Academy of Sciences of the United States of America 101, 13642-7.
Phanse, Y., Ramer-Tait, A.E., Friend, S.L., Carrillo-Conde, B., Lueth, P., Oster, C.J., Phillips, G.J., Narasimhan, B., Wannemuehler, M.J. and Bellaire, B.H., 2012, Analyzing cellular internalization of nanoparticles and bacteria by multi-spectral imaging flow cytometry. Journal of visualized experiments : JoVE, e3884.
Ploppa, A., George, T.C., Unertl, K.E., Nohe, B. and Durieux, M.E., 2011, ImageStream cytometry extends the analysis of phagocytosis and oxidative burst. Scandinavian journal of clinical and laboratory investigation 71, 362-9.
Purdy, G.E., 2011, Taking Out TB-Lysosomal Trafficking and Mycobactericidal Ubiquitin-Derived Peptides. Frontiers in microbiology 2, 7.
Rohde, K., Yates, R.M., Purdy, G.E. and Russell, D.G., 2007, Mycobacterium tuberculosis and the environment within the phagosome. Immunological reviews 219, 37-54.
Russell, D.G., 2011, Mycobacterium tuberculosis and the intimate discourse of a chronic infection. Immunological reviews 240, 252-68.
Smirnov, A., Solga, M.D., Lannigan, J. and Criss, A.K., 2015, An improved method for differentiating cell-bound from internalized particles by imaging flow cytometry. Journal of immunological methods 423, 60-9.
Sturgill-Koszycki, S., Schlesinger, P.H., Chakraborty, P., Haddix, P.L., Collins, H.L., Fok, A.K., Allen, R.D., Gluck, S.L., Heuser, J. and Russell, D.G., 1994, Lack of acidification in Mycobacterium phagosomes produced by exclusion of the vesicular proton-ATPase. Science 263, 678-81.
Sun-Wada, G.H., Tabata, H., Kawamura, N., Aoyama, M. and Wada, Y., 2009, Direct recruitment of H+-ATPase from lysosomes for phagosomal acidification. J Cell Sci 122, 2504-13.
Theus, S.A., Cave, M.D. and Eisenach, K.D., 2004, Activated THP-1 cells: an attractive model for the assessment of intracellular growth rates of Mycobacterium tuberculosis isolates. Infection and immunity 72, 1169-73.
van der Wel, N., Hava, D., Houben, D., Fluitsma, D., van Zon, M., Pierson, J., Brenner, M. and Peters, P.J., 2007, M. tuberculosis and M. leprae translocate from the phagolysosome to the cytosol in myeloid cells. Cell 129, 1287-98.
Vergne, I., Chua, J., Singh, S.B. and Deretic, V., 2004, Cell biology of mycobacterium tuberculosis phagosome. Annu Rev Cell Dev Biol 20, 367-94.

Verrall, A.J., Netea, M.G., Alisjahbana, B., Hill, P.C. and van Crevel, R., 2014, Early clearance of Mycobacterium tuberculosis: a new frontier in prevention. Immunology 141, 506-13.
Via, L.E., Deretic, D., Ulmer, R.J., Hibler, N.S., Huber, L.A. and Deretic, V., 1997, Arrest of mycobacterial phagosome maturation is caused by a block in vesicle fusion between stages controlled by rab5 and rab7. The Journal of biological chemistry 272, 13326-31.
von Bargen, K., Polidori, M., Becken, U., Huth, G., Prescott, J.F. and Haas, A., 2009, Rhodococcus equi virulence-associated protein A is required for diversion of phagosome biogenesis but not for cytotoxicity. Infection and immunity 77, 5676-81.
Welin, A., Amirbeagi, F., Christenson, K., Bjorkman, L., Bjornsdottir, H., Forsman, H., Dahlgren, C., Karlsson, A. and Bylund, J., 2013, The Human Neutrophil Subsets Defined by the Presence or Absence of OLFM4 Both Transmigrate into Tissue In Vivo and Give Rise to Distinct NETs In Vitro. PloS one 8, e69575.
Welin, A., Eklund, D., Stendahl, O. and Lerm, M., 2011a, Human macrophages infected with a high burden of ESAT-6-expressing M. tuberculosis undergo caspase-1- and cathepsin B-independent necrosis. PloS one 6, e20302.
Welin, A. and Lerm, M., 2012, Inside or outside the phagosome? The controversy of the intracellular localization of Mycobacterium tuberculosis. Tuberculosis 92, 113-20.
Welin, A., Raffetseder, J., Eklund, D., Stendahl, O. and Lerm, M., 2011b, Importance of phagosomal functionality for growth restriction of Mycobacterium tuberculosis in primary human macrophages. Journal of innate immunity 3, 508-18.
Welin, A., Winberg, M.E., Abdalla, H., Sarndahl, E., Rasmusson, B., Stendahl, O. and Lerm, M., 2008, Incorporation of Mycobacterium tuberculosis lipoarabinomannan into macrophage membrane rafts is a prerequisite for the phagosomal maturation block. Infection and immunity 76, 2882-7.
Zimmerli, S., Edwards, S. and Ernst, J.D., 1996, Selective receptor blockade during phagocytosis does not alter the survival and growth of Mycobacterium tuberculosis in human macrophages. Am J Respir Cell Mol Biol 15, 760-70.

Figure legends

Figure 1. IDEAS analysis of phagocytosis. THP-1 cells were infected with H37Ra-GFP at a ratio of 2:1 for 2 h, stained with LysoTracker, and analyzed by imaging flow cytometry. A four-step gating strategy was employed to identify and quantify the proportion of cells that had bound and/or internalized phagocytic prey. Sequential IDEAS plots (numbered) and gates are shown, as well as examples of cells that were included and excluded by the gates in each step (arrows). The title of each plot indicates which population is being displayed, carrying over from the gated population in the previous plot. Brightfield images are shown in greyscale, GFP is shown in green, and LysoTracker in red.

Figure 2. Phagocytosis measurements. A) THP-1 cells were allowed to phagocytose unopsonized or serum-opsonized (50 % serum) zymosan-FITC at a ratio of 1:1 for 2 h, stained for CD63, and analyzed for phagocytosis. **B)** THP-1 cells were allowed to phagocytose serum-opsonized (50 % serum) zymosan-FITC at a ratio of 1:1 for the indicated times, stained for CD63, and analyzed for phagocytosis. **C)** THP-1 cells were infected with unopsonized, serum (25 % serum)- or IgG-opsonized H37Ra-GFP at a ratio of 2:1 for 2 h, stained with LysoTracker, and analyzed for phagocytosis. The proportions of cells with prey bound to the cell surface (grey) and internalized (white) are shown in the bar graphs. The means ± SD of 4 (A and C) or 3 (B) independent experiments are shown. Differences in phagocytosis were analyzed using two-way repeated measures ANOVA followed by Holm-Sidak's multiple comparison test (A and C). Asterisks indicate significant differences in internalization.

Figure 3. IDEAS analysis of phagosome maturation: Phagosome maturation score. THP-1 cells were allowed to phagocytose H37Ra-GFP (M.tb) at a ratio of 2:1 (A-C, E) or zymosan-FITC at a ratio of 1:1 (D) for 2 h, stained with LysoTracker (A-C, E) or for CD63 (D), and analyzed by imaging flow cytometry. **A)** A two-step gating strategy subsequent to that shown in Fig. 1 was employed to identify the cells that could be analyzed for phagosome maturation. Sequential IDEAS plots (numbered) and gates are shown, as well as examples of cells that were included and excluded by the gates in each step (arrows). The title of each plot indicates which population is being displayed. Brightfield images are shown in greyscale and GFP in green. **B)** The masking strategy with LysoTracker (red) and GFP (green) images, and the masks for the phagosome and remainder of the cell (overlain in cyan and highlighted with dotted lines), is shown. **C)** A histogram of the phagosome maturation scores with examples of cells that were included or excluded by the gate for mature phagosomes are shown (arrows), with GFP in green and LysoTracker in red. **D)** A histogram of the phagosome maturation scores with examples of cells that were included or excluded by the gate for mature phagosomes are shown (arrows), with FITC in green and CD63 in red. **E)** Phagosome maturation in H37Ra-GFP-infected and LysoTracker (LT)-stained cells was analyzed through manual scoring of the first 100 images containing a cell with a single phagosome, or by using the phagosome maturation score. The bar graph shows the mean proportion of mature phagosomes ± SD from the same 3 independent experiments using the two methods of quantification.

Figure 4. IDEAS analysis of phagosome maturation: Colocalization. THP-1 cells were infected with H37Ra-GFP at a ratio of 2:1 for 2 h, stained with LysoTracker (LT), and analyzed by imaging flow cytometry. The histogram shows bright detail similarity scores from a representative sample, and example images (arrows) depict cells with high and low scores, respectively. Overlain images of LysoTracker (red) and GFP (green) are shown.

Figure 5. Phagosome maturation measurements. A) THP-1 cells were infected with heat-killed FITC-labeled H37Ra or live H37Ra-GFP at a ratio of 2:1 for 2 h, stained with LysoTracker (LT), and analyzed for phagosome maturation by imaging flow cytometry. The proportion of cells that contained a mature phagosome based on the phagosome maturation score is shown in the left bar graph, while the right bar graph depicts the median bright detail similarity scores in the same samples. **B)** THP-1 cells were infected with unopsonized heat-killed FITC-labeled H37Ra, unopsonized live H37Ra-GFP, or serum (25 % serum)- or IgG-opsonized live H37Ra-GFP at a ratio of 2:1 for 2 h, stained with LysoTracker (LT), and analyzed for phagosome maturation by imaging flow cytometry. The proportion of cells that contained a mature phagosome based on the phagosome maturation score is shown in the left bar graph, while the right bar graph depicts the median bright detail similarity scores in the same samples. **C)** THP-1 cells were infected with FITC-labeled zymosan particles at a ratio of 1:1 for different periods of time, stained for CD63, and analyzed for phagosome maturation by imaging flow cytometry (phagosome maturation score). **D)** THP-1 cells were infected with FITC-labeled zymosan particles or live H37Ra-GFP at a ratio of 1:1 for 2 h, stained for CD63, and analyzed for phagosome maturation by imaging flow cytometry (phagosome maturation score). In C-D, the bar graphs show the proportion of cells that contained a mature phagosome. The means ± SD of 5 (A and D), 3 (C), or 4 (B) independent experiments are shown. Differences in phagosome maturation were analyzed using paired Student's t-test (A and D) or ordinary one-way ANOVA followed by Holm-Sidak's multiple comparison test (B).

Figure 6. IDEAS analysis of bacterial numbers. THP-1 cells were infected with H37Ra-GFP (M.tb) at a ratio of 2:1 for 2 h, stained for CD63, and analyzed by imaging flow cytometry using the EDF option. **A)** The masking strategy with CD63 (red) and GFP (green) images, and the mask for the prey (white), is shown. **B)** A histogram of the bacterial count feature in the prey-containing population and examples of cells that were determined by the analysis to contain 0, 1, 2, or 3 cells are shown. The images show overlays of GFP (green) and CD63 (red). **C)** A histogram of the number of bacteria per cell as determined by manual inspection of the first 300 images, in the prey-containing population, from the same sample as depicted in (B) is shown.

Figure 7. Intracellular bacterial replication measurements. THP-1 cells were infected with H37Ra-GFP at a ratio of 2:1 for the indicated times, in the presence (squares) or absence (circles) of 100 µg/ml streptomycin. The cells were then stained for CD63 and the mean number of bacteria per cell (in the single cell-population) was analyzed by imaging flow cytometry with the EDF option. Means ± SEM from 3 independent experiments are shown. Differences in bacterial numbers after 96 h were analyzed using paired Student's t-test.

Figure 8. Workflow and possible analyses. The numbered list (left panel) and flow chart (right) show the steps involved in the presented imaging flow cytometry-based analyses of phagocytosis, phagosome maturation, and bacterial replication, as well as which analyses are possible in the same sample depending on the instrument settings. EDF refers to the extended depth of field option on the ImageStreamX, and as depicted in the right panel the same sample can be run both with (1) and without (2) this option.

Fig. 1

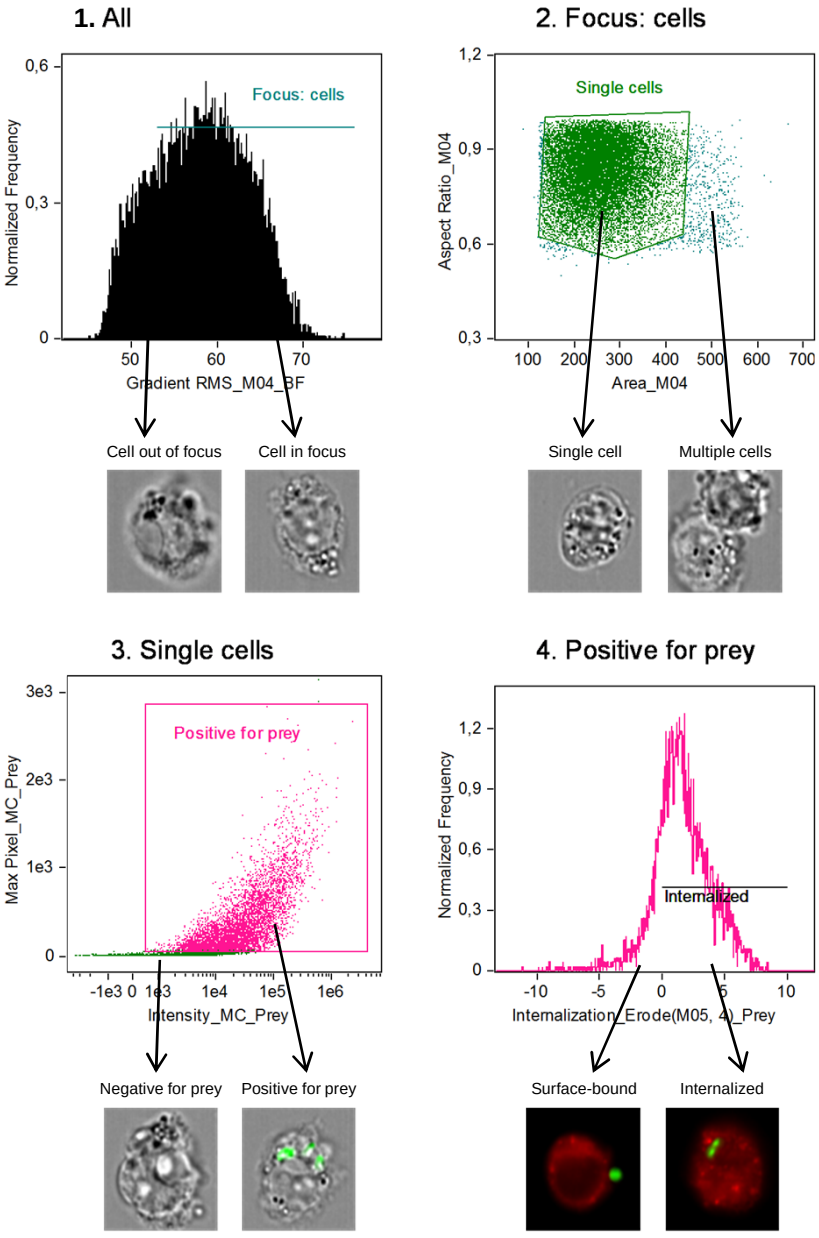
1. All
Focus: cells
Normalized Frequency
Gradient RMS_M04_BF
Cell out of focus
Cell in focus
2. Focus: cells
Single cells
Aspect Ratio_M04
Area_M04
Single cell
Multiple cells
3. Single cells
Positive for prey
Max Pixel_MC_Prey
Intensity_MC_Prey
Negative for prey
Positive for prey
4. Positive for prey
Internalized
Normalized Frequency
Surface-bound
Internalized

Fig. 2

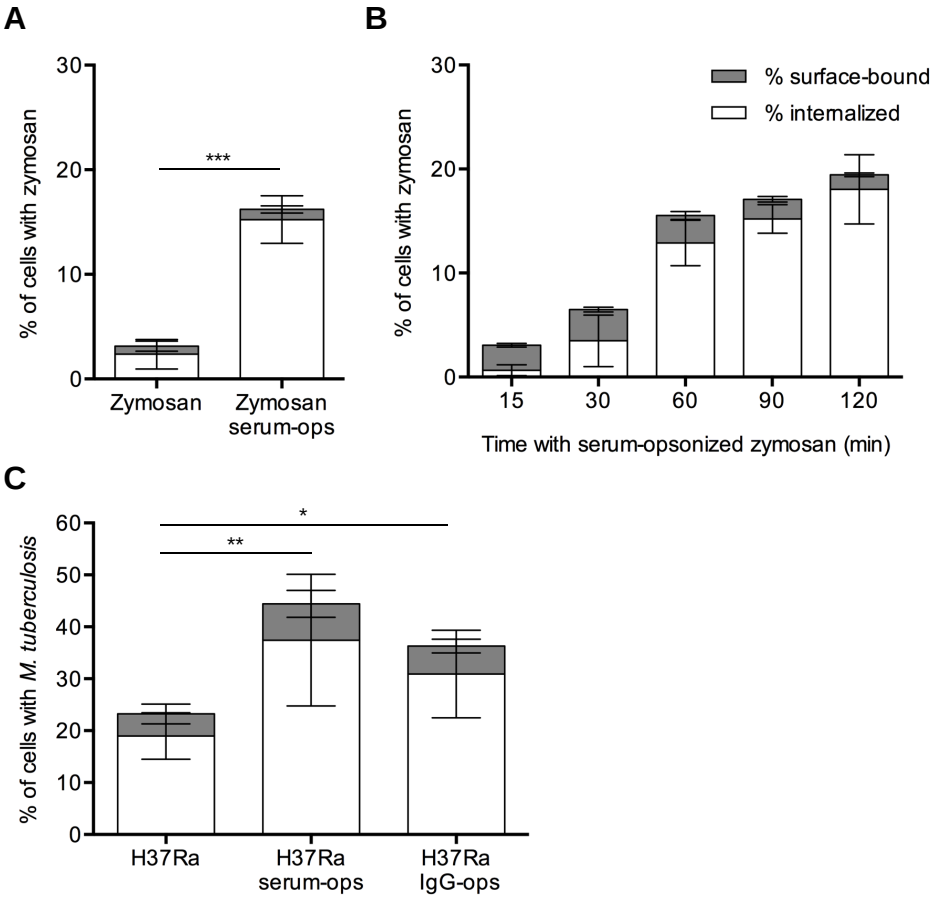
A
B
C
% of cells with zymosan
***
Zymosan
Zymosan serum-ops
% surface-bound
% internalized
Time with serum-opsonized zymosan (min)
15
30
60
90
120
% of cells with M. tuberculosis
*
**
H37Ra
H37Ra serum-ops
H37Ra IgG-ops

Fig. 3

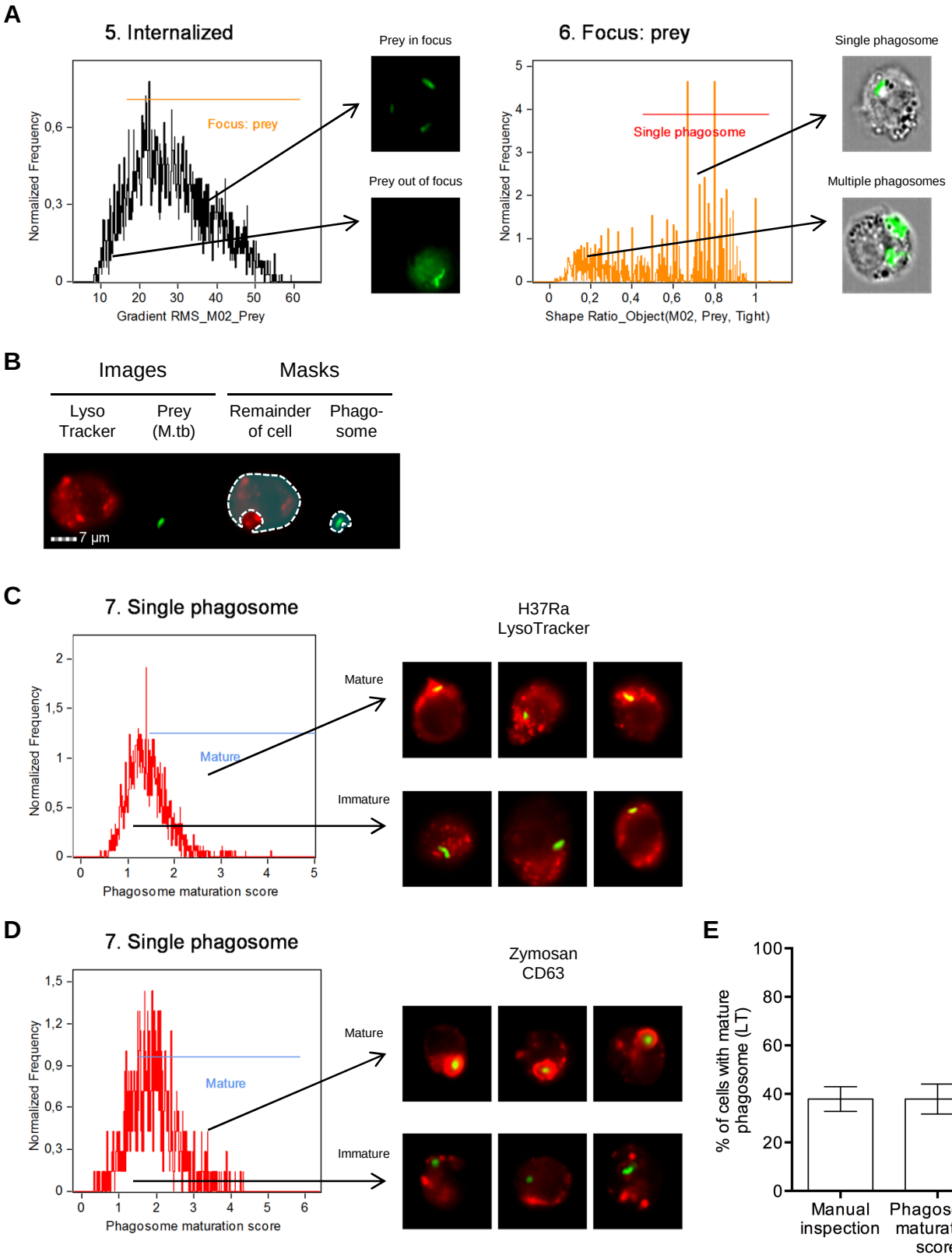
A
5. Internalized
Prey in focus
Prey out of focus
Focus: prey
Normalized Frequency
Gradient RMS_M02_Prey
6. Focus: prey
Single phagosome
Multiple phagosomes
Single phagosome
Shape Ratio_Object(M02, Prey, Tight)
B
Images
Masks
Lyso Tracker
Prey (M.tb)
Remainder of cell
Phago-some
7 µm
C
7. Single phagosome
H37Ra LysoTracker
Mature
Immature
Mature
Normalized Frequency
Phagosome maturation score
D
7. Single phagosome
Zymosan CD63
Mature
Immature
Mature
Normalized Frequency
Phagosome maturation score
E
% of cells with mature phagosome (LT)
Manual inspection
Phagosome maturation score

Fig. 4

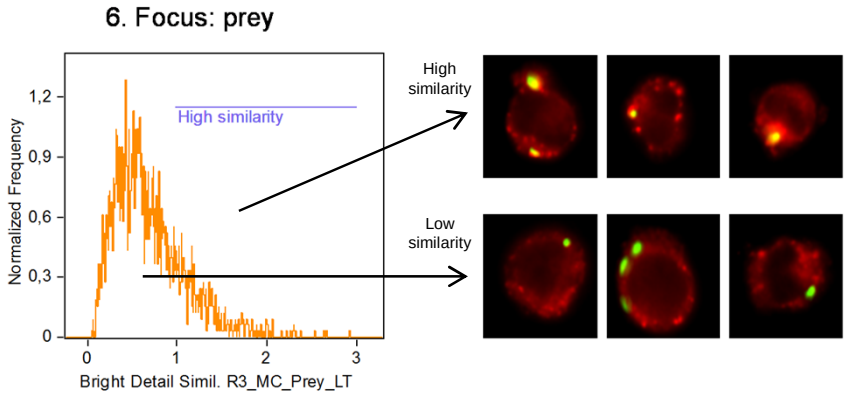
6. Focus: prey
High similarity
Normalized Frequency
1,2
0,9
0,6
0,3
0
0
1
2
3
Bright Detail Simil. R3_MC_Prey_LT
High similarity
Low similarity

Fig. 5

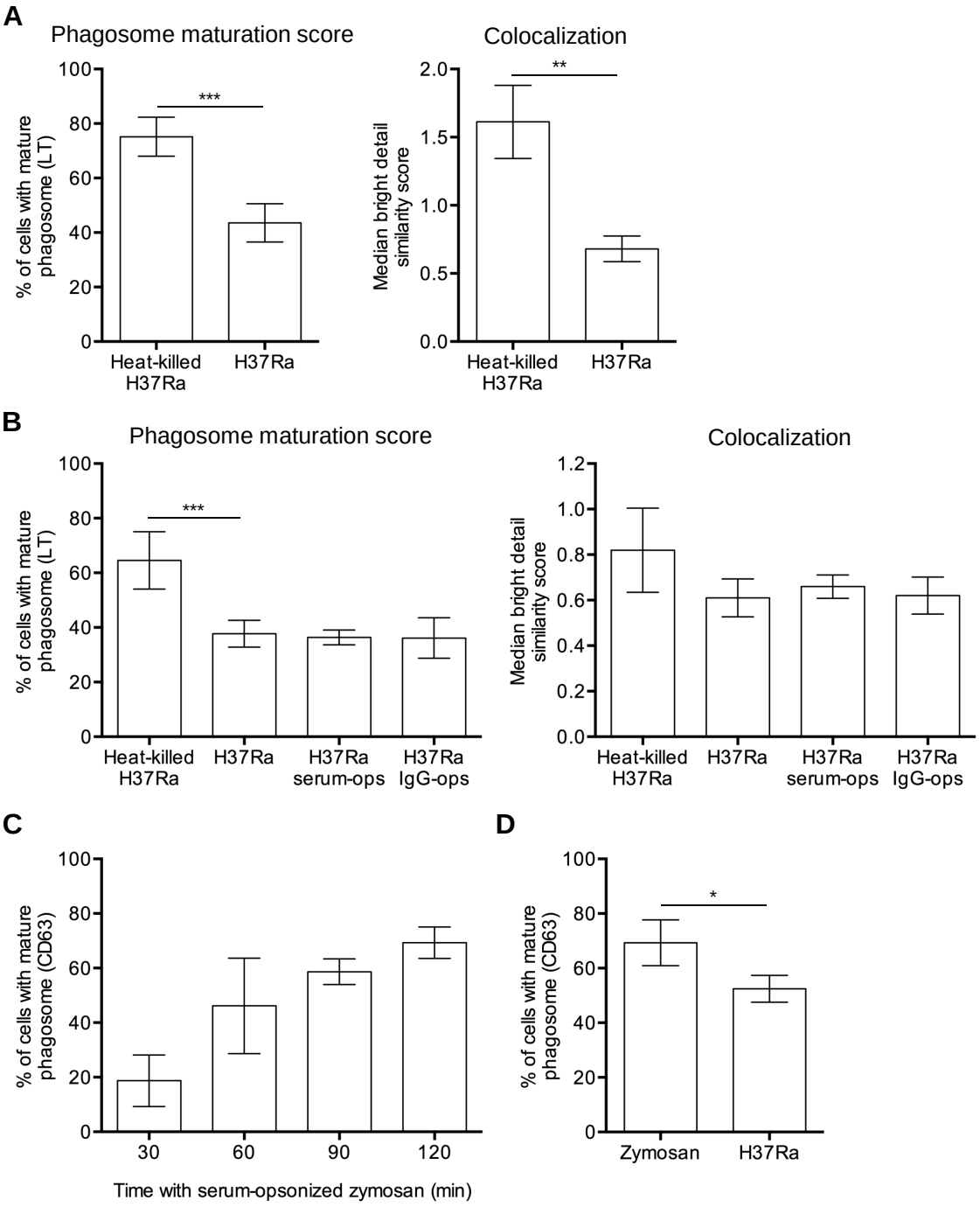
A
Phagosome maturation score
% of cells with mature phagosome (LT)
100
80
60
40
20
0
***
Heat-killed H37Ra
H37Ra
Colocalization
Median bright detail similarity score
2.0
1.5
1.0
0.5
0.0
**
Heat-killed H37Ra
H37Ra
B
Phagosome maturation score
% of cells with mature phagosome (LT)
***
Heat-killed H37Ra
H37Ra
H37Ra serum-ops
H37Ra IgG-ops
Colocalization
Median bright detail similarity score
1.2
1.0
0.8
0.6
0.4
0.2
0.0
Heat-killed H37Ra
H37Ra
H37Ra serum-ops
H37Ra IgG-ops
C
% of cells with mature phagosome (CD63)
100
80
60
40
20
0
30
60
90
120
Time with serum-opsonized zymosan (min)
D
% of cells with mature phagosome (CD63)
*
Zymosan
H37Ra

Fig. 6

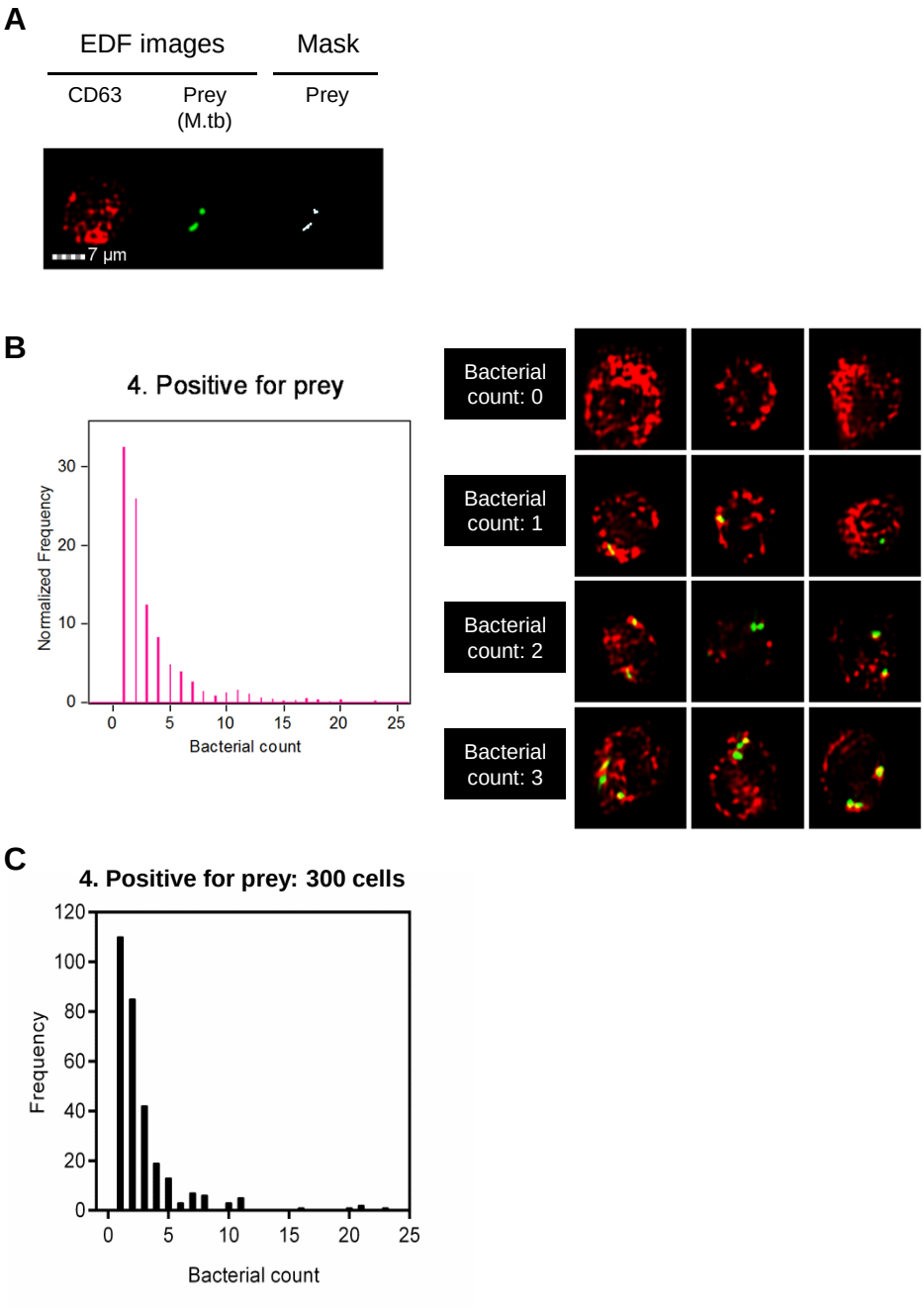
A
EDF images
Mask
CD63
Prey (M.tb)
Prey
7 µm
B
4. Positive for prey
Normalized Frequency
Bacterial count
Bacterial count: 0
Bacterial count: 1
Bacterial count: 2
Bacterial count: 3
C
4. Positive for prey: 300 cells
Frequency
Bacterial count

Fig. 7

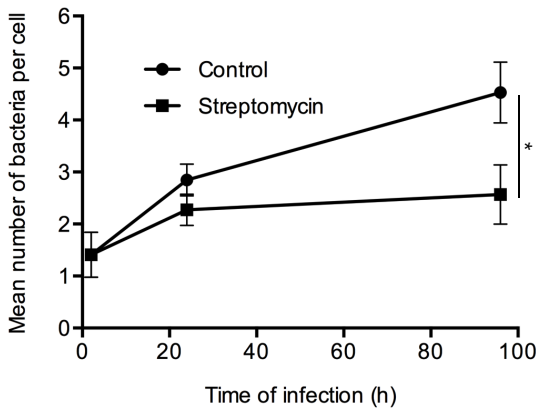
Mean number of bacteria per cell
0
1
2
3
4
5
6
Control
Streptomycin
*
0
20
40
60
80
100
Time of infection (h)

Fig. 8

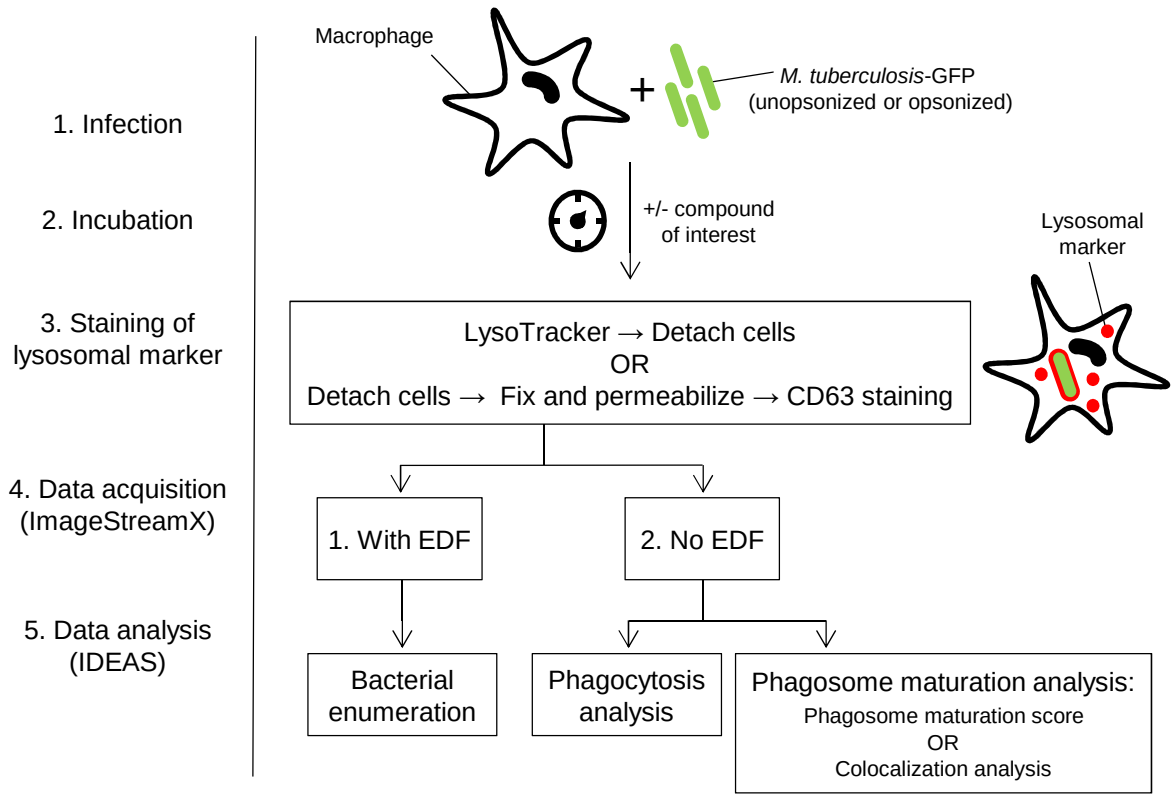
1. Infection
2. Incubation
3. Staining of lysosomal marker
4. Data acquisition (ImageStreamX)
5. Data analysis (IDEAS)
Macrophage
+
M. tuberculosis-GFP
(unopsonized or opsonized)
+/- compound of interest
Lysosomal marker
LysoTracker → Detach cells
OR
Detach cells → Fix and permeabilize → CD63 staining
1. With EDF
2. No EDF
Bacterial enumeration
Phagocytosis analysis
Phagosome maturation analysis:
Phagosome maturation score
OR
Colocalization analysis